Relationship between Snow Extent and Midlatitude Disturbance Centers

MATTHEW RYDZIK AND ANKUR R. DESAI

Department of Atmospheric and Oceanic Sciences, University of Wisconsin—Madison, Madison, Wisconsin

(Manuscript received 28 November 2012, in final form 2 January 2014)

ABSTRACT

A relationship between midlatitude cyclone (MLC) tracks and snow-cover extent has been discussed in the literature over the last 50 years but not explicitly analyzed with high-resolution and long-term observations of both. Large-scale modeling studies have hinted that areas near the edge of the snow extent support enhanced baroclinicity because of differences in surface albedo and moisture fluxes. In this study, the relationship between snow-cover extent and midlatitude disturbance (MLD) trajectories is investigated across North America using objectively analyzed midlatitude disturbance trajectories and snow-cover extent from the North American Regional Reanalysis (NARR) for 1979–2010. MLDs include low-level mesoscale disturbances through midlatitude cyclones. A high-resolution MLD database is developed from sea level pressure minima that are tracked through subsequent 3-h time steps, and a simple algorithm is developed that identified the southern edge of the snow-cover extent. A robust enhanced frequency of MLDs in a region 50–350 km south of the snow-cover extent is found. The region of enhanced MLD frequency coincides with the region of maximum low-level baroclinicity. These observations support hypotheses of an internal feedback in which the snow-cover extent is leading the disturbance tracks through surface heat and moisture fluxes. Further, these results aid in the understanding of how midlatitude disturbance tracks may shift in a changing climate in response to snow-cover trends.

1. Introduction

Trajectories of midlatitude disturbances (MLDs) are important for both climate and weather prediction because they have a direct impact on societal weather hazards. MLDs include closed low pressure systems ranging from low-level mesoscale disturbances through midlatitude cyclones (MLCs). MLCs are primarily driven by large-scale forcing such as upper-level jets and baroclinic instability, while midlatitude disturbances can be driven by mesoscale features. It can be argued, however, that boundary layer forcing may play a role in some MLC trajectories by the modulation of boundary layer thermodynamics (Namias 1962). Past individual case studies have been useful for showing the mechanistic process by which the boundary layer modulates free-troposphere dynamics, but only long-term and large-spatial-scale statistical analysis can determine how common and significant these processes are across all MLCs and MLDs. A relationship between snow-cover extent and MLCs has been discussed in the literature for almost 50 years; however, it has not been explicitly analyzed with high-resolution and long-term observations of both.

Namias (1962) was one of the first to suggest a direct relationship between MLC trajectories and preexisting snow cover. Using the abnormal southern extent of snow from February to March 1960, Namias (1962) estimated expected surface air temperature given midlevel geopotential height and showed that the largest difference between this estimated surface temperature and observed surface temperature occurred along the southern edge of the snow extent, with the difference reaching up to 5.6°C. The difference elsewhere, away from the snow-cover extent, was minimal. The estimated surface temperature used by Namias (1962) is the temperature expected given 700-hPa height based on multiple regression equations of Klein et al. (1959). The finding suggested that snow cover significantly affected lower tropospheric temperature near the snow-extent boundary in a way that is colder than what would be expected given the midlevel temperature profile. The cooler profile at low levels suggests enhanced gradients in that region. Namias (1962) then postulated that enhanced baroclinicity near

Corresponding author address: Matthew Rydzik, 1225 W. Dayton Street, Madison, WI 53706.
E-mail: matthew.rydzik@gmail.com

DOI: 10.1175/JCLI-D-12-00841.1

the edge of the snow extent can lead to a positive reinforcement of the temperature contrast (and thus baroclinicity) because of developing MLCs within this region. Namias (1978) cited a similar mechanism of enhanced baroclinicity near the U.S. East Coast attributable to anomalous snow cover for the winter of 1976/77. Similarly, Ross and Walsh (1986) found that inland snow played a role in MLC paths, but it is not known how often this occurred because the study was limited to storms that had trajectories parallel to and within 500–600 km of the snow-extent boundary.

Model simulations have had conflicting findings relative to these observational studies with regards to trajectories. Elguindi et al. (2005) modified snow cover under observed MLCs using a mesoscale model [fifth-generation Pennsylvania State University–National Center for Atmospheric Research Mesoscale Model (MM5)] in the Great Plains. Using two simulations, one with observed snow cover and one in which the entire inner model domain was snow covered, they found that there was little and inconsistent change to MLC trajectories. The MLCs in their simulations weakened because the snow cover removed a significant portion of the energy from the land surface (Elguindi et al. 2005). These findings were used to argue against Namias (1962)'s postulation that the snow-cover extent boundary can have an effect on MLC trajectories. However, it is important to note that, by filling the entire domain with snow, the MLC was no longer near the snow-cover boundary that both Namias (1962) and Ross and Walsh (1986) postulated was necessary for a positive feedback mechanism owing to a region of enhanced baroclinicity. The work of Elguindi et al. (2005) demonstrated the importance of snow cover to the energetics of MLCs by finding decreased intensities when the entire inner domain was snow covered.

More recent model and statistical analysis has shown that the effect of North American snow cover on large-scale circulation patterns is not negligible (Klingaman et al. 2008; Leathers et al. 2002; Sobolowski et al. 2007). The results of Klingaman et al. (2008) suggest that 1) snow cover in the Great Plains added positively to the North Atlantic Oscillation index, influencing European climate and 2) regional changes in snow cover have a larger impact than continental snow-cover changes. The work of Sobolowski et al. (2010) further showed a transient eddy response to an anomalous snow forcing and that the response was a result of enhanced baroclinicity in existing storm-track entrance regions of the North Atlantic. The same investigators more recently presented that the largest driver of the stationary wave response attributable to anomalous snow cover is the diabatic cooling from increased snow cover (Sobolowski et al. 2011).

More frequent and widespread observations and advances in reanalysis products allow us to now take a closer look at the relationship between snow cover and MLDs. In this manuscript, we used the North American Regional Reanalysis (NARR) to 1) identify snow-cover extent and MLDs and 2) assess the relationship between the two. The previous studies investigated the relationship between storms known to exist along the edge of the snow extent, but an unanswered question remains: how common are MLDs near the snow-extent edge?

We hypothesize that the snow-extent boundary will be a preferential region for MLD centers because of increased low-level baroclinicity. The enhanced low-level baroclinicity will mainly be driven by the enhanced temperature gradient across the boundary from snow-covered to bare ground because of differences in surface energy balance.

2. Data and methods

A high-temporal- and spatial-resolution analysis is needed in order to understand the synoptic and mesoscale processes that are involved in land–atmosphere coupling because MLC identification and tracking can be masked at coarser temporal and spatial resolutions (Blender and Schubert 2000). To meet these requirements and to maintain a physically consistent relationship between snow on the ground and the atmosphere, the NARR was used. In this section we describe the NARR and methods (snow-cover extent, MLD identification, MLD tracking, and low-level baroclinicity) used to investigate the relationship between MLD trajectories and snow-cover extent.

a. North American Regional Reanalysis

The NARR is a high-spatial- and temporal-resolution reanalysis dataset for North America from 1979 to the present (Mesinger et al. 2006). NARR has a horizontal grid spacing of approximately 32 km and consists of 47 layers in the vertical. NARR snow depth (SNOD) and pressure at mean sea level (PRMSL) network common data form (netCDF) files were obtained from the website of the National Oceanic and Atmospheric Administration (NOAA)/Office of Oceanic and Atmospheric Research (OAR)/Earth System Research Laboratory (ESRL) Physical Sciences Division (PSD), Boulder, Colorado (available at http://www.esrl.noaa.gov/psd/). NARR uses the Noah land surface model to simulate the snowpack. The snow–water equivalent base state is updated at 0000 UTC using the U.S. Air Force snow depth (SNODEP) model (Mesinger et al. 2006).

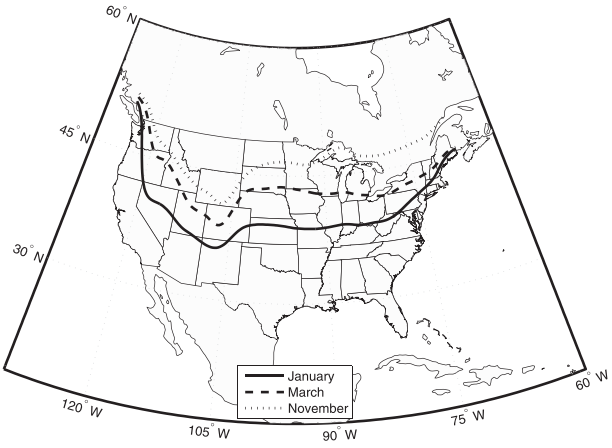

FIG. 1. Mean longitudinally varying latitude of continuous snow cover for January, March, and November.

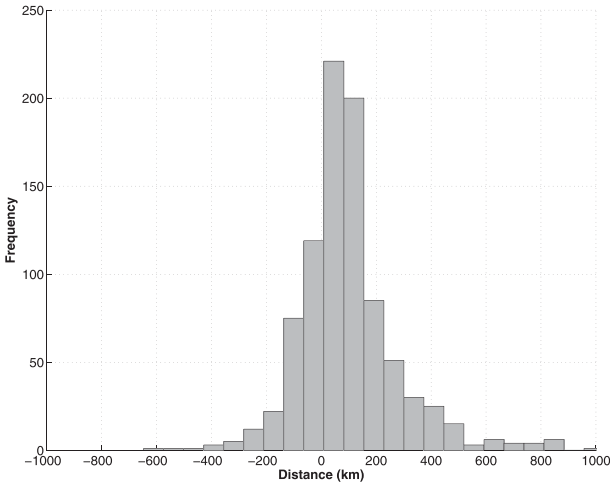

FIG. 2. The mean difference between NARR and SNODAS snow-cover extent per day for 2004–09 from November to March. NARR tends to be farther north than SNODAS, but the overall agreement is acceptable.

b. *Snow-cover extent*

Snow-cover extent was objectively determined from NARR snow depth using a simple algorithm that located the longitudinally varying southern extent of continuous snow cover across North America. For a given day, the snow-extent analysis was limited to 0000 UTC because NARR tends to exhibit an unrealistic variation in snow cover throughout the day (National Centers for Environmental Prediction 2012). The snow depth was converted to a categorical snow cover and linearly interpolated to a 0.25° grid spanning 10°–80°N and 130°–62°W. Grid points that have snow at some location in each cardinal direction were set to be covered. The algorithm then searched each longitude point, from south to north, looking for 10 consecutive snow-covered points (equal to 2.5°). When 10 consecutive snow-covered points were found, the snow extent was set to the first (most southern) point in the snow-covered region. After finding the latitude of snow-cover extent at each longitude bin, the line was further smoothed with a 10-point running mean filter. The mean latitude of the longitudinally varying snow cover for January, March, and November is shown in Fig. 1. A comparison between NARR and the Snow Data Assimilation System (SNODAS) snow-cover extent is presented in Fig. 2 for the years 2004–09 during the months of November–March. SNODAS combines satellite, airborne, and ground stations to estimate snow cover (National Operational Hydrologic Remote Sensing Center 2012). The largest differences tend to occur over mountainous regions.

c. *Midlatitude disturbance trajectories*

MLD trajectories were identified by finding a local minimum in NARR sea level pressure and tracking it at subsequent time steps. The following approach is similar to Serreze et al. (1997) with regards to identification and tracking, but it incorporates a combination of identification at two resolutions. It is important to note that our tracking scheme does not impose a low-end-duration cutoff or minimum depth; therefore, the scheme identifies both low-level mesoscale disturbances and midlatitude cyclones. A concern of relying solely on MSLP is that weak systems may be masked by the large-scale pattern and that MSLP is an extrapolated field (Hoskins and Hodges 2002). The sea level pressure field at each time step was linearly interpolated to two grids with spacing of 0.25° (fine) to provide a common grid for analysis and 2.5° (coarse) to aid in our MLD identification algorithm. The coarse resolution was chosen to be 2.5° because it removed most of the noise in the MSLP field that was resulting in spurious MLD identifications, especially in mountainous regions. The interpolated grids cover the region from 20° to 65°N and from 155° to 60°W in order to allow adequate space from the domain edges for the local minimum finding to be reliable. Mathematical critical points (derivative equal to zero) at both grid spacings were found by identifying the intersection of the zero derivative contours for both the east–west and the north–south orientations. Local minima were identified by finding where the second derivatives in both the east–west and north–south orientations were greater than zero (concave up). The coarse-resolution identifications were then refined by changing their location to the nearest fine-resolution minimum. Relating the coarse resolution to the fine resolution was done to improve the accuracy of the coarse resolution and to ignore the fine-resolution noise that typically appeared

in mountainous regions. Tracking of MLD was performed using a nearest-neighbor method to link pressure minimum together into coherent storms over time derived from the algorithm of Chandler and Jonas (2012) and similar to the work of Serreze et al. (1997). At subsequent 3-hourly time steps, storms were searched within a radius of 361 km of the current storm position (120 km hr^{-1}). To prevent pressure minima from unrealistically backtracking, future pressure minima must be located in a region generally to the east of the previous location (between compass angles 355° and 185°). Pressure minimum identified as being part of a storm were not used in future searches. In the case when no pressure minimum was found within the search radius, the search radius was doubled and the 6-h pressure field was searched. If a pressure minimum was not found at the 6-h time step, then the storm ends. If in any 6-h period a storm has not moved more than 0.25°, then the track was terminated. The entire database consisted of 6702 MLDs over 32 years for storms lasting at least 1 day.

d. Low-level baroclinicity

The commonly suggested mechanism for why there should be a relationship between snow-cover extent and MLC tracks is the existence of a region with enhanced low-level baroclinicity near the snow-cover extent. To investigate this, we developed a measure of low-level baroclinicity. A common measure of baroclinic instability is (Hoskins and Valdes 1990; Lindzen and Farrell 1980)

$$\sigma_{\mathrm{BI}} = 0.31 \frac{f}{N} \frac{dV}{dz}, \tag{1}$$

where f is the Coriolis parameter, N is the Brunt–Väisälä frequency, V is the horizontal wind, and z is height. The metric σ_{BI} is a measure of the growth rate of a baroclinic wave and is sometimes referred to as the eddy growth rate (Long et al. 2009). Equation (1) can be rearranged and discretized as

$$\sigma_{\mathrm{BI}} = 0.31 \frac{f}{\sqrt{\dfrac{g}{\Theta_m} \dfrac{\Theta_u - \Theta_l}{\Phi_u - \Phi_l}}} \left| \frac{V_u - V_l}{\Phi_u - \Phi_l} \right|, \tag{2}$$

where Θ_l, Θ_m, and Θ_u are the potential temperature at the lower, middle, and upper levels; Φ_l, Φ_m, and Φ_u are the geopotential height at the lower, middle, and upper levels; and V_l and V_u are the magnitude of the wind at the lower and upper levels For the low-level baroclinicity calculation, the lower level for the discretization was defined as being the first NARR pressure level that was at least 150 hPa less than the surface pressure, the middle level for the discretization was the next NARR modeled pressure level (lower pressure and higher altitude), and the upper level for the discretization was defined as the next NARR modeled pressure level at a higher altitude (less pressure) than the middle pressure level. The eddy growth rate was then linearly interpolated to the 0.25° spacing used for all other calculations and analysis.

Using the aforementioned process, low-level baroclinicity over North America was typically calculated at a pressure level ranging from 800 hPa over low topography up to 550 hPa in high topography. The typical bottom layer for the discretization was just above the boundary layer at approximately 155–190 hPa above the surface (~1–2 km). The layers on which low-level baroclinicity were calculated remain relatively constant throughout the year and rarely varied by more than two model pressure levels.

e. Statistical analysis

Unless otherwise noted, all analyses were performed for 0000 UTC 1 January 1978–2100 UTC 31 December 2010. Over this time period, the distance from each center, for all identified centers in a MLD track, to the nearest snow-cover extent point was calculated using the snow cover and MLD position on the same day (zero lag) and for lags from −5 to +5 days. The MLD center is the identified minima in the mean sea level pressure field. If the MLD center was over snow, then the distance value is set to be negative. The distance was calculated for all months, except for June through September, which were removed because, during the summer and early fall, the snow extent approached the northern edge of our domain. We do not have confidence in the results when the snow extent is near the edge of our domain because of the inability of our algorithm and model to properly simulate snow cover at domain edges.

The results are discussed with relation to three seasons: fall, winter, and spring. November is presented as the representative member of the fall (October and November), January is presented as winter (December–February), and March is presented as spring (March–May). To investigate the significance of any enhanced peaks, 31 additional distance distributions were calculated using the snow cover from the 31 other years. The resulting distributions were then subtracted from the distribution using snow cover and MLD centers in the same year. Summing the differences between all the distributions shows where the most consistent anomalies of snow cover and MLD occurred in that particular year. It is assumed that shuffling the data will create mostly random noise that will cancel when summed.

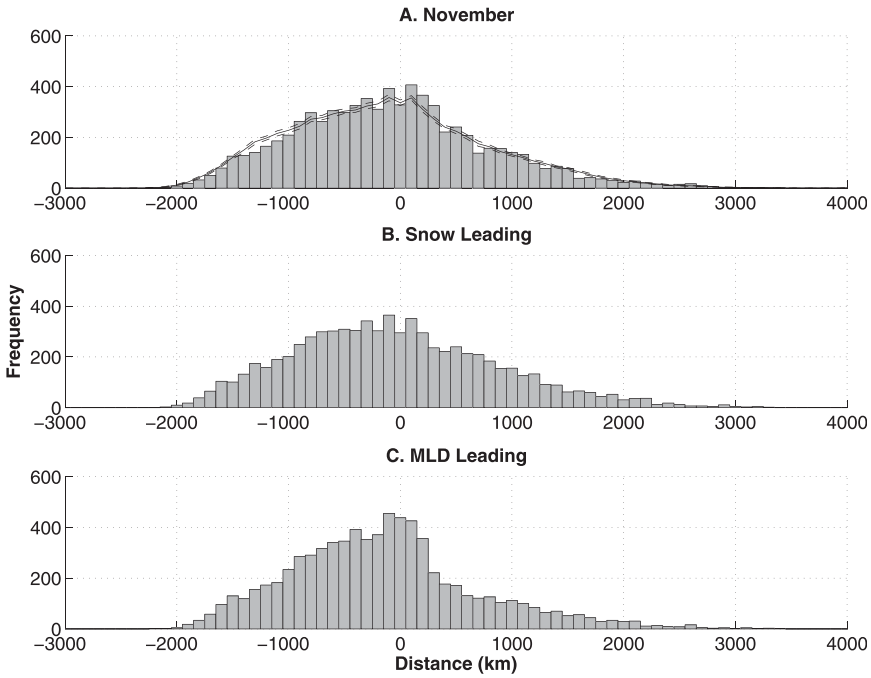

FIG. 3. MLD center distance from snow-cover extent for storms lasting longer than 24 h using various lags in November for 1979–2010. Negative distances are MLD centers that are over snow, and positive distances are MLD centers that are over ground without snow. (a) MLD cyclone frequency peaks in a region south of the snow-cover extent for snow cover and MLDs on the same day. The shuffled mean and 99% confidence interval are shown by lines in (a). (b) There is little change if snow cover is leading the MLDs by 2 days, suggesting that preexisting snow cover plays a role in the relationship. (c) A shift to the left, consistent with snow being deposited by the storm itself, is seen when the MLD leads the snow cover by 2 days.

In addition, 99% confidence intervals, using a two-tailed Student's *t* test, were calculated for each bin of the distribution using the 32 distributions (31 shuffled and 1 not shuffled).

Further, to investigate the magnitude of gradients in boundary layer forcing across the snow-cover extent, composite plots of albedo, latent heat flux, sensible heat flux, and 2-m temperature relative to the snow-cover extent were computed for the month of March.

3. Results

a. Relationship

Our initial analysis was limited to storms that last at least 24 h in order to remove the weakest MLDs in our database that are likely not significant events. A histogram of the distance between the snow extent and the MLD centers for fall (Fig. 3a) shows the center of the distribution to be related to the snow-extent line (zero distance). The maximum frequency occurs just south of the snow-extent line and exhibits a longer tail south of the snow extent than to the north. January (winter) has a bimodal distribution with a peak near the snow-extent line and another peak approximately 450–750 km north of the snow-extent line (Fig. 4a). Possible explanations for the peak north of the snow extent are presented in the discussion. The spring has a distribution that is very similar to the fall (Fig. 5a). The main difference in March is a more pronounced peak in frequency just south of the snow-extent line. The enhanced peak in frequency is about 50–350 km south of the snow-extent line. The tail south of the snow-extent line is not as large as November, but the frequency north of the snow-extent line retains its shape with only a small increase in magnitude. The common trait among all months is an enhanced frequency of MLDs in a region 50–350 km south of the snow-extent line.

There is approximately a 35% reduction in the number of MLD centers and 25% reduction in the number of MLDs when requiring storms to last at least 48 h as compared to 24 h. For these longer-lived storms, the distance between the MLD center and the snow-cover extent in the fall does not have as pronounced peak as seen in storms lasting longer than a day. The same is true for the winter with no enhanced peaks and, in addition, the distributions are centered on a region approximately

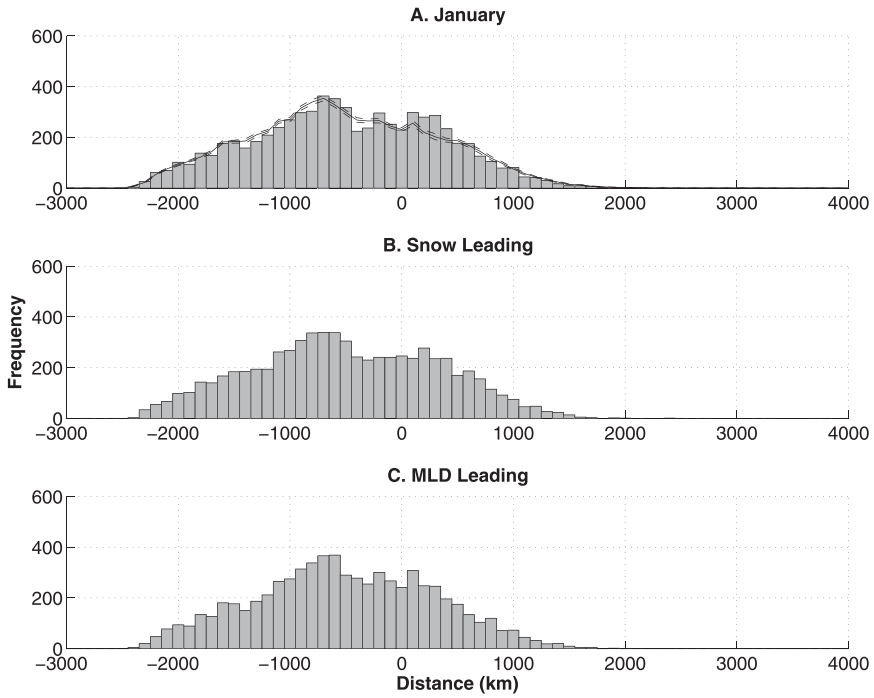

FIG. 4. MLD center distance from snow-cover extent for storms lasting longer than 24 h using various lags in January for 1979–2010. Negative distances are MLD centers that are over snow, and positive distances are MLD centers that are over ground without snow. (a) MLDs are most frequent about 700 km north of the snow-cover extent and about 50–350 km south of the snow-cover extent. The shuffled mean and 99% confidence interval are shown by lines in (a). The lagged relationship of (b) snow cover leading the MLDs and (c) the MLDs leading the snow cover by 2 days is consistent with the other seasons (Figs. 3, 5).

500 km north of the snow extent. The spring season still exhibits an enhancement of MLD center frequency in a region of 50–350 km south of the snow-extent line. April and May exhibit stronger peaks than March (not shown).

Reducing the minimum duration to only 9 h substantially increases the number of MLDs. In the fall, there is enhanced frequency of MLD centers near the snow-extent line in a region 0–200 km south of the snow extent. The region is slightly farther north than storms lasting longer than 1 day. The distribution shows a higher frequency of MLD centers south of the snow extent and the frequency does not decay as rapidly as compared to storms lasting longer than a day. The winter distributions are very similar to their 24-h counterparts. There is a bimodal distribution with one peak in a region 100–300 km south of the snow extent and another peak in a region 600–800 km north of the snow extent. Spring continues to show an enhanced peak 100–300 km south of the snow-extent line as it has for all three MLD longevity criteria. However, the drop in frequency south of the enhanced region is not as steep as the longer-duration storms.

Comparing the distribution for the actual year to all other years with our shuffling analysis shows the largest and most coherent structures in a region just south of the snow-extent line (Fig. 6). There are substantial differences in the distributions just south of the snow-extent line when using snow-cover extent from all other years. Further, the peaks south of the snow-cover extent are much above the 99% confidence interval (Figs. 3a, 4a, 5a). There is a significant increased frequency of MLD centers in a region 50–350 km south of the extent line when the snow-cover extent and MLDs are from the same year.

b. *Lagged relationship*

For the remainder of the analysis, we focus on storms that last longer than a day because they exhibit the strongest relationship between the snow-cover extent and the location of the MLD center. It can be argued that one would expect a relationship between MLD tracks and snow-cover extent because during the cold season it is generally anticipated that snow would be produced on the northern side of MLDs. Therefore, one may expect to see MLDs track just south of the snow

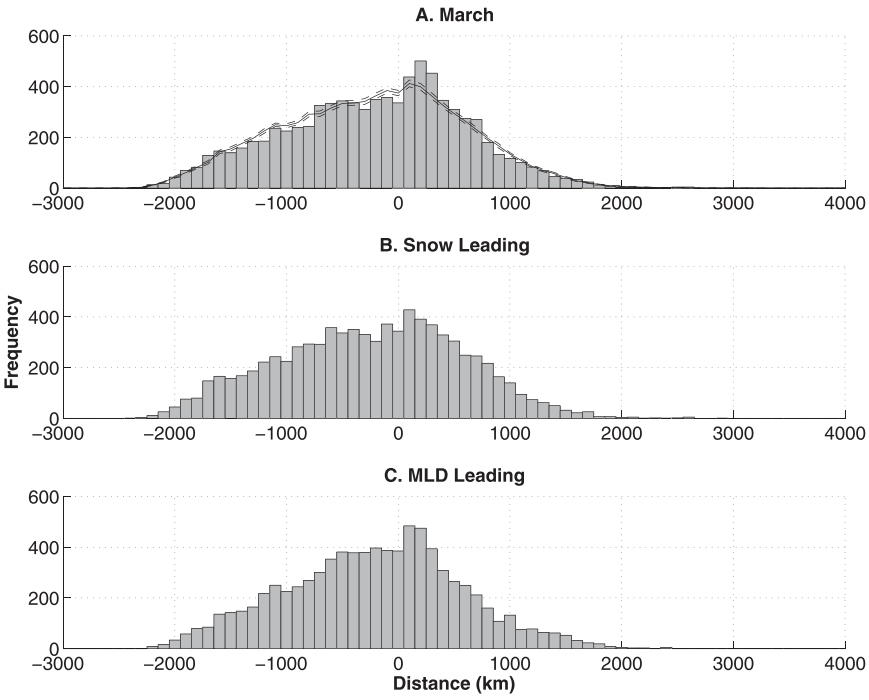

FIG. 5. MLD center distance from snow-cover extent for storms lasting longer than 24 h using various lags in March for 1979–2010. Negative distances are MLD centers that are over snow, and positive distances are MLD centers that are over ground without snow. (a) MLD cyclone frequency exhibits a stronger peak south of the snow-cover extent than in November for snow cover and MLDs on the same day. The shuffled mean and 99% confidence interval are shown by lines in (a). (b) Snow cover leading the MLDs by 2 days and (c) MLDs leading the snow cover by 2 days show the similar and expected response as previously seen in November (Fig. 3).

extent when using no lag time. To investigate if this is an issue, lagged relationships were looked at with both snow-cover extent and MLD leading.

The results suggest that it is preexisting snow cover that is related to the MLD tracks and this is shown in middle and bottom panels of Figs. 3–5. A 2-day lag with snow cover leading is representative of snow cover leading for lags 1–5. There is very little difference between the 0-day lag and the other lag times with snow leading. With the snow cover leading the MLDs there is still an enhanced frequency of MLD centers in a region approximately 50–350 km south of the snow-extent line. There is a small shift to left observed in a few months. A strong leftward shift is seen with MLDs leading the snow-cover extent by 2 days. In November, with the MLDs leading the snow cover, the mean shifts from −43 to −73 km and the skewness shows a shift to the left (0.47–0.65). The skewness for January and March also confirm a shift to the left, from 0 to 0.04 and from −0.02 to 0.04, respectively. The peaks with MLDs leading also tend to be larger, more pronounced, and nearly centered on zero distance.

c. *Low-level baroclinicity*

Normalized mean low-level baroclinicity in 100-km bins surrounding the snow extent are presented in Fig. 7. It is evident that baroclinicity peaks in a region just south of the snow extent in all months. The structure of baroclinicity is almost identical for all months with the smallest values in a region approximately 1500 km south of the snow extent and the largest values occurring in a region from the snow extent to approximately 1000 km south of the snow extent. The fall (Fig. 7a) has a stronger peak than the other months because of much lower baroclinicity values north of the snow extent as compared to the winter and spring. The largest values of low-level baroclinicity occur in a region that roughly coincides with the peaks in MLD frequency. It is important to note that the enhancement of baroclinicity is much broader and not as pronounced at the MLD distance distribution peaks.

Plots of select variables (albedo, temperature, latent heat flux, and sensible heat flux) relative to the snow-cover extent are shown in Fig. 8 for the month of March.

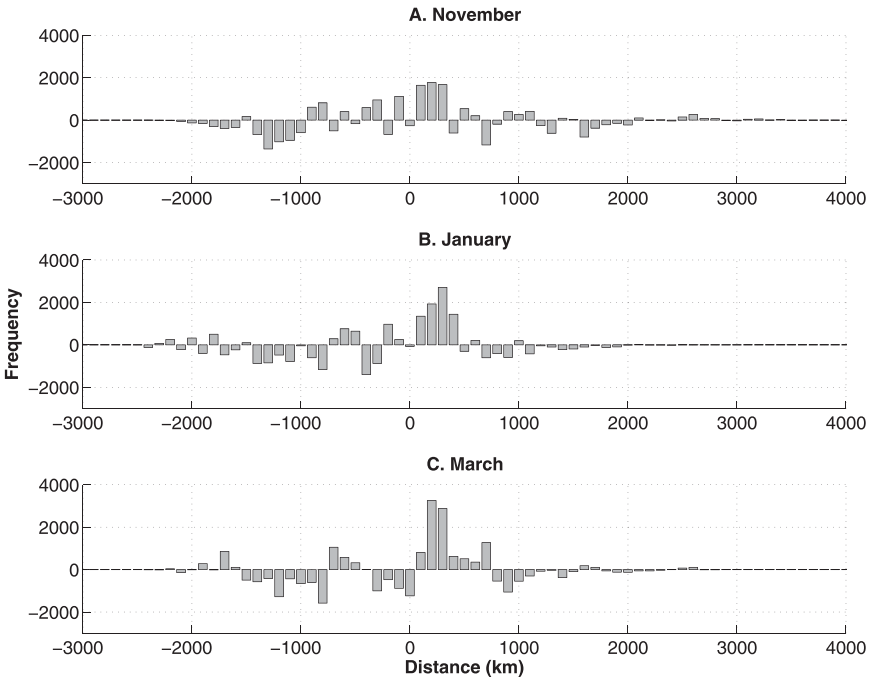

FIG. 6. The sum of the differences between the distributions of the MLD center and snow-cover extent using snow from the same year and all other years. Large peaks show regions where the MLD frequency is closely tied to the snow-cover extent for a particular year.

The values represent composite mean daily values for each variable following the snow-cover extent on each day. There is clear difference in albedo across the snow-extent boundary (Fig. 8a) as expected with values north of the snow extent averaging between 35% and 55% and values south of the snow extent in the 15%–25% range. The smaller-scale structures in the albedo are tied to mountains and vegetation. The expected temperature structure relative to the snow extent is seen and shown in Fig. 8b. There is a small enhancement of temperature gradient near the snow-cover extent. Snow cover tends to mute the sensible (Fig. 8c) and latent heat (Fig. 8d) fluxes as compared to bare ground, and they exhibit a structure that is related to the snow cover–extent edge. The difference in sensible and latent heat fluxes is consistent with a temperature anomaly pattern supportive of enhanced baroclinic instability.

4. Discussion

We found a statistically robust enhanced frequency of MLDs in a region 50–350 km south of the snow extent over the 32-yr reanalysis of snow cover and MLD trajectories. The region of enhanced MLD frequency is also the region where the largest values of low-level baroclinicity are experienced. Below, we discuss the structure of these features more fully and use them to add evidence to a postulation that snow-cover extent may play a role in the northward shift of storm tracks seen under conditions of anthropogenic climate change (ACC).

a. Statistical robustness

There is a strong and robust relationship of the distance between MLD centers and the southern edge of the snow-cover extent. The frequency distribution of MLD centers typically featured enhanced peaks in a region south of the snow extent for storms lasting longer than 1 day and all the distributions are nearly centered near the snow-extent line. A preferential region for MLD trajectories near the snow-extent boundary supports the ideas postulated in Namias (1962) and studied further in Ross and Walsh (1986) that snow cover can have an impact on MLC trajectories. However, we showed that the snow-cover feedback is likely to have a larger impact on disturbances that may not be MLCs, and therefore we cannot say that snow cover is changing MLC trajectories. From the aforementioned results, the preferential region can be quantified as likely being 50–350 km south of the snow extent.

The bimodal distributions seen in a few months (mainly January) can plausibly be explained by Alberta clippers. Alberta clippers are fast-moving low pressure systems that are most commonly found in December and January (Thomas and Martin 2007). Alberta clippers are generated in the lee of the Rocky Mountains in Alberta, Canada, and generally track east-southeast

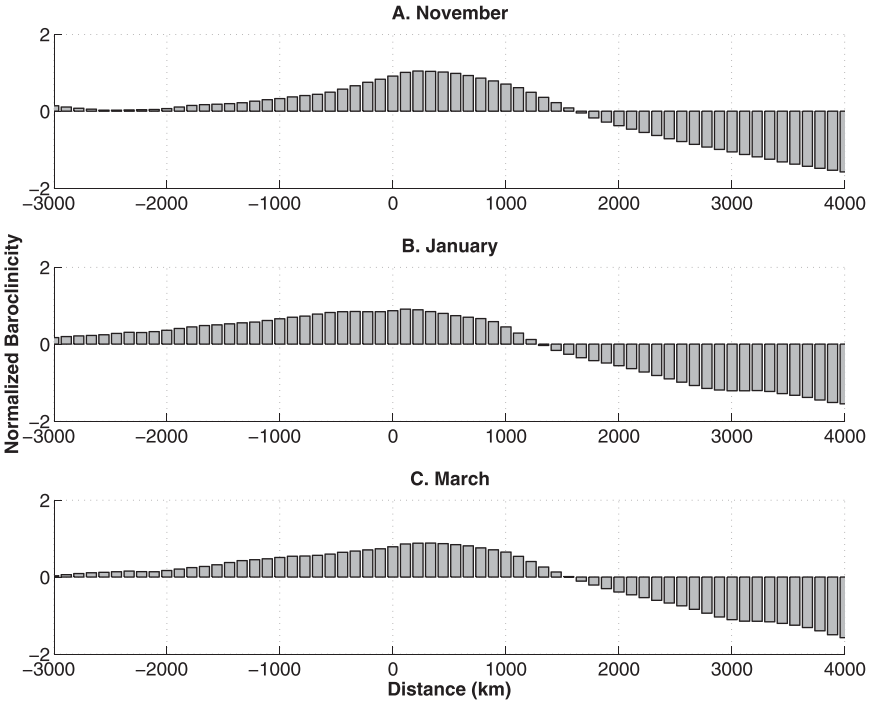

FIG. 7. Normalized low-level baroclinicity relative to the snow-cover extent for (a) November, (b) January, and (c) March. Low-level baroclinicity peaks in the region south of the snow-cover extent where MLDs are most frequent.

toward the north-central border of the United States, where they then continue to progress eastward (Thomas and Martin 2007). The trajectory of an average Alberta clipper is approximately 600–800 km north of the mean January snow extent (~40°N). This region corresponds to the location of the bimodal peak observed north of the snow over extent in January. The fast-moving nature of these storms is the reason the bimodal peak becomes less pronounced, as the minimum duration of MLDs increases and more pronounced when only requiring that storms last at least 9 h.

As previously noted, it can be argued that a close relationship between MLDs and snow-cover extent is expected because winter MLDs are likely to deposit snow. Lagged analysis shows that it is preexisting snow cover that is related to the MLD trajectories. The differences between snow cover and MLDs on the same day versus snow cover 2 days before the MLDs are small. This is highly suggestive that it is not snow being produced by the MLD itself. In addition, the relationship with the MLD leading the snow cover is consistent with the expectation of snow being produced to the north of the center and nonfrozen precipitation to the south. With the MLDs leading the snow cover by 2 days there is a shift toward the left in the distributions, indicative of the center moving closer to the snow edge. This is likely snow deposited by the MLD itself.

It is difficult to determine the significance of the enhanced peaks near the snow extent because there is no a priori expected distribution from which to compare. To attempt to prove the enhanced peaks near the snow extent are significant and not a random occurrence, we computed distributions of the distance between snow-cover extent and MLDs using snow cover from all other years as a way to shuffle the datasets. Summing the distributions should result in any random noise canceling out. The most coherent structures in the differences occur in a region 50–350 km south of the snow extent. Outside of the region south of the boundary, the structures in the differences are not coherent and are of smaller magnitude. The peaks are also significant at the 99% confidence level and exhibit a value much larger than the upper limit of the confidence interval. The structures suggest that MLDs in the region just south of the boundary are closely tied to the snow-cover extent for the same year. Therefore, the relationship between MLD centers and the snow-cover extent must have a physical link.

b. Physical mechanisms and seasonal differences

We also noted that the strongest relationship is found in spring. The peaks observed in the distributions of distances are largest and the robustness analysis has the largest and most coherent structures during this season.

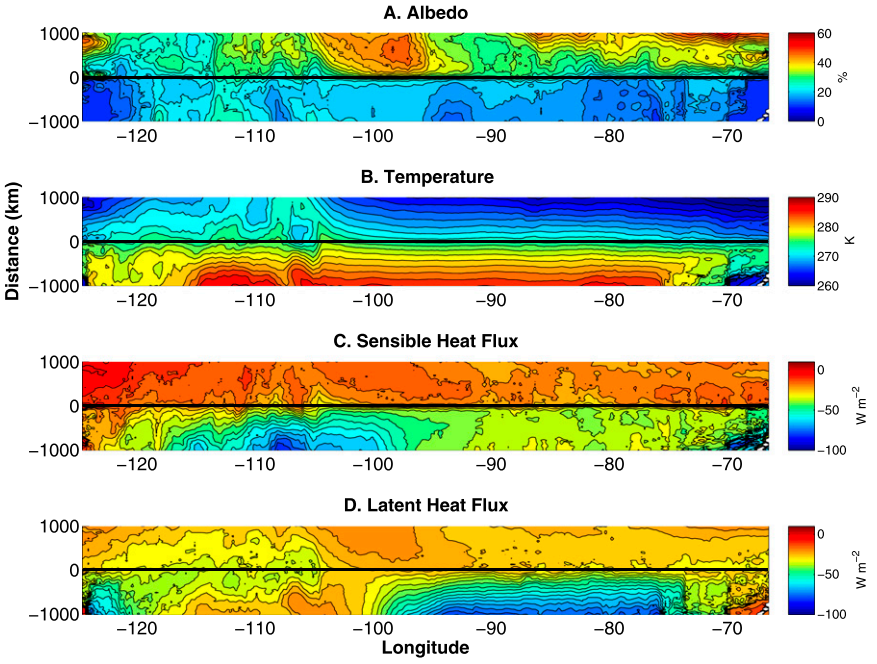

FIG. 8. Gradients of select variables relative to the snow-cover extent (black line): (a) surface albedo (%), (b) 2-m air temperature (K), (c) sensible heat flux ($W\,m^{-2}$), and (d) latent heat flux ($W\,m^{-2}$). Negative fluxes are from the surface to the atmosphere. The strong gradients seen relative to the snow-cover extent will result in significantly varying boundary layers. These boundary layer effects may propagate upward and affect MLD tracks.

This result may be attributed to increasing incident solar radiation during the spring. The increase in solar radiation will in turn increase the temperature contrast between the snow-covered ground and the bare ground, which we observed in our temperature and albedo gradient maps. Segal et al. (1991) similarly found that the ''snow breeze'' was strongest during the spring for this very reason. A ''snow breeze'' type of circulation and increasing solar radiation resulting in a temperature contrast are two physical processes that can link the snow-cover extent to the MLDs. As additional evidence toward robustness of the result, the snow extent–MLD relationship is similar to the distributions seen using the Atlas of Extratropical Storm Tracks (Chandler and Jonas 2012) instead of our NARR-derived storm positions.

It is important to remember that there are large-scale circulation influences on MLDs. The results suggest that it is most likely that shorter-duration MLDs (mostly low-level mesoscale disturbances) have a stronger relationship with preexisting snow cover than longer MLDs (more likely to be MLCs) that are likely a result of the large-scale circulation pattern and instability. The stronger peaks seen with shorter-duration MLDs suggest that the magnitude of the temperature gradient across the snow cover–extent edge is comparable with other forcing factors.

The commonly postulated (e.g., Namias 1962; Ross and Walsh 1986) mechanism for the relationship between MLC tracks and snow-cover extent is one that is based on a region of enhanced low-level baroclinicity along the snow-cover extent. The enhanced temperature and moisture gradient setup from the change in surface properties induces a temperature gradient between the snow-covered ground and the ground without snow cover. The temperature gradient is a result of a large gradient in surface albedo that leads to a large difference in absorbed incident solar radiation. The increased temperature gradient across the snow-extent line is then believed to lead to enhanced low-level baroclinicity. Regions of enhanced baroclinicity are more favorable for MLDs because the eddy growth rate is enhanced. Our results show that the largest mean baroclinicity values, relative to the snow extent, are in a region just south of the snow extent.

The area of enhanced baroclinicity is much broader (from approximately the snow extent to 800 km south of the snow extent) than the peaks observed in MLD cycle frequency relative to the snow extent that tended to be very pronounced and limited to a few hundred kilometers. The region of largest baroclinicity just south of the snow extent provides support for the mechanism proposed in Namias (1962) and Ross and Walsh (1986). The

region immediately south of the snow extent will experience maximum eddy growth rates making it a region that is favorable for MLDs to develop and grow. The region of maximum growth rate is analogous to the region of maximum baroclinic instability. It is expected that MLDs will tend to follow regions of maximum baroclinic instability because it is the primary driving mechanism for them and this is what is seen in the results. The region of maximum eddy growth rate is coincident with the region of maximum frequency of MLDs.

Our analysis is unable to provide a mechanism for how this low-level baroclinicity is realized at upper levels. We speculate that a preexisting disturbance at upper levels is needed in order to realize the enhanced baroclinicity at low levels. The low-level baroclinicity will modify the structure of the MLD resulting in trajectory changes. More work is needed to understand why the MLD centers are seen in a region 50–350 km south of the snow extent while the region of maximum baroclinic instability does not always peak in that region and has a much broader structure.

c. *Impact of future climatic change*

With ACC, snow-cover extent is anticipated to decrease (Brown and Mote 2009) because of rising global temperatures. If the relationship between MLD centers and snow-cover extent remains constant with ACC, then a northward shift of MLDs over continents would be expected given a shift northward in snow-cover extent. Our results indicate that it may only be weaker storms that see a shift resulting from retreating snow-cover extent. Stronger storms, which are shown to exhibit a weaker relationship, would likely be driven by the large-scale circulation. Therefore, it is unlikely that the snow-cover feedback is driving any shifts in the storm track, but the snow cover can play a role in reinforcing any shifts that occur because of changes in large-scale circulation patterns. MLCs have been shown to exhibit complex spatial and temporal variations (Zhang et al. 2004) and that makes it difficult to determine the role snow cover has played in any historical variation.

5. Conclusions

An MLD identification and tracking method was developed using high-temporal- and spatial-resolution NARR output. A simple algorithm for determining the southern extent of snow cover in North America was created so the MLD centers could be compared to it. Investigation of the role snow-cover extent has on MLD trajectories showed that there is an enhanced region of MLD frequency 50–350 km south of the snow-cover extent. The relationship appears to be driven by low-level baroclinicity that is at its maximum in this region. Increased low-level baroclinicity is thought to be driven by the increased temperature gradient across the boundary because of differences in absorbed solar radiation. The relationship between MLD centers and snow-cover extent is shown to be robust by shuffling years of snow cover and showing that the largest and most coherent changes occur in the region of enhanced MLD frequency and that the peaks exceed the 99% confidence limits. The close relationship between MLD centers and snow-cover extent may play a role in the storm-track changes with ACC by reinforcing large-scale circulation changes and steering weaker disturbances. Snow cover is found to lead the MLD centers; thus, with a northward retreat of snow-cover extent resulting from ACC, we expect a similar northward shift in MLD centers over the North American continent. An expected shift in MLC tracks cannot be discerned because of a weakening relationship between snow cover and MLDs with increasing storm duration.

Further modeling studies, similar to the work of Elguindi et al. (2005), would aid in the understanding of the physical link between the snow cover and MLD. It is important in these studies to keep the snow perturbations realistic to prevent the MLD center from becoming too far separated from the snow-cover extent boundary, where there is enhanced low-level baroclinicity. Expanding the statistical analysis performed here to Europe and Asia along with using more reanalysis products would add more confidence to our results. A better understanding of the physical processes involved will allow for a better assessment of what changes to MLD trajectories can be expected with ACC.

Acknowledgments. The work was funded by the USA Department of Energy's 20% by 2030 Award DE-EE0000544/001, titled "Integration of Wind Energy Systems into Power Engineering Education Programs at UW–Madison." We thank the two anonymous reviewers, whose comments greatly improved the quality of this paper and helped us present our findings more clearly.

REFERENCES

Blender, R., and M. Schubert, 2000: Cyclone tracking in different spatial and temporal resolutions. *Mon. Wea. Rev.,* **128,** 377–384, doi:10.1175/1520-0493(2000)128<0377:CTIDSA>2.0.CO;2.

Brown, R. D., and P. W. Mote, 2009: The response of Northern Hemisphere snow cover to a changing climate. *J. Climate,* **22,** 2124–2145, doi:10.1175/2008JCLI2665.1.

Chandler, M., and J. Jonas, cited 2012: Atlas of extratropical storm tracks (1961-1998). [Available online at http://www.giss.nasa.gov/data/stormtracks.]

Elguindi, N., B. Hanson, and D. Leathers, 2005: The effects of snow cover on midlatitude cyclones in the Great Plains. *J. Hydrometeor.,* **6,** 263–279, doi:10.1175/JHM415.1.

Hoskins, B. J., and P. J. Valdes, 1990: On the existence of storm-tracks. *J. Atmos. Sci.,* **47,** 1854–1864, doi:10.1175/1520-0469(1990)047<1854:OTEOST>2.0.CO;2.

——, and K. I. Hodges, 2002: New perspectives on the Northern Hemisphere winter storm tracks. *J. Atmos. Sci.,* **59,** 1041–1061, doi:10.1175/1520-0469(2002)059<1041:NPOTNH>2.0.CO;2.

Klein, W. H., B. M. Lewis, and I. Enger, 1959: Objective prediction of five-day mean temperatures during winter. *J. Meteor.,* **16,** 672–682, doi:10.1175/1520-0469(1959)016<0672:OPOFDM>2.0.CO;2.

Klingaman, N. P., B. Hanson, and D. J. Leathers, 2008: A teleconnection between forced Great Plains snow cover and European winter climate. *J. Climate,* **21,** 2466–2483, doi:10.1175/2007JCLI1672.1.

Leathers, D. J., T. L. Mote, A. J. Grundstein, D. A. Robinson, K. Felter, K. Conrad, and L. Sedywitz, 2002: Associations between continental-scale snow cover anomalies and air mass frequencies across eastern North America. *Int. J. Climatol.,* **22,** 1473–1494, doi:10.1002/joc.807.

Lindzen, R. S., and B. Farrell, 1980: A simple approximate result for the maximum growth rate of baroclinic instabilities. *J. Atmos. Sci.,* **37,** 1648–1654, doi:10.1175/1520-0469(1980)037<1648:ASARFT>2.0.CO;2.

Long, Z., W. Perrie, J. Gyakum, R. Laprise, and D. Caya, 2009: Scenario changes in the climatology of winter midlatitude cyclone activity over eastern North America and the Northwest Atlantic. *J. Geophys. Res.,* **114,** D12111, doi:10.1029/2008JD010869.

Mesinger, F., and Coauthors, 2006: North American Regional Reanalysis. *Bull. Amer. Meteor. Soc.,* **87,** 343–360, doi:10.1175/BAMS-87-3-343.

Namias, J., 1962: Influences of abnormal heat sources and sinks on atmospheric behavior. *Proc. Int. Symp. on Numerical Weather Prediction,* Tokyo, Japan, Meteorological Society of Japan, 615–627.

——, 1978: Multiple causes of the North American abnormal winter 1976–77. *Mon. Wea. Rev.,* **106,** 279–295, doi:10.1175/1520-0493(1978)106<0279:MCOTNA>2.0.CO;2.

National Centers for Environmental Prediction, cited 2012: Regional reanalysis questions and answers. [Available online at http://www.emc.ncep.noaa.gov/mmb/rreanl/faq.html.]

National Operational Hydrologic Remote Sensing Center, cited 2012: Snow Data Assimilation System (SNODAS) data products at NSIDC. [Available online at http://nsidc.org/data/docs/noaa/g02158_snodas_snow_cover_model/.]

Ross, B., and J. E. Walsh, 1986: Synoptic-scale influences of snow cover and sea ice. *Mon. Wea. Rev.,* **114,** 1795–1810, doi:10.1175/1520-0493(1986)114<1795:SSIOSC>2.0.CO;2.

Segal, M., J. R. Garratt, R. A. Pielke, and Z. Ye, 1991: Scaling and numerical model evaluation of snow-cover effects on the generation and modification of daytime mesoscale circulations. *J. Atmos. Sci.,* **48,** 1024–1042, doi:10.1175/1520-0469(1991)048<1024:SANMEO>2.0.CO;2.

Serreze, M. C., F. Carse, and R. Barry, 1997: Icelandic low cyclone activity: Climatological features, linkages with the NAO, and relationships with recent changes in the Northern Hemisphere circulation. *J. Climate,* **10,** 453–464, doi:10.1175/1520-0442(1997)010<0453:ILCACF>2.0.CO;2.

Sobolowski, S., G. Gong, and M. Ting, 2007: Northern Hemisphere winter climate variability: Response to North American snow cover anomalies and orography. *Geophys. Res. Lett.,* **34,** L16825, doi:10.1029/2007GL030573.

——, ——, and ——, 2010: Modeled climate state and dynamic responses to anomalous North American snow cover. *J. Climate,* **23,** 785–799, doi:10.1175/2009JCLI3219.1.

——, ——, and ——, 2011: Investigating the linear and nonlinear stationary wave response to anomalous North American snow cover. *J. Atmos. Sci.,* **68,** 904–917, doi:10.1175/2010JAS3581.1.

Thomas, B. C., and J. E. Martin, 2007: A synoptic climatology and composite analysis of the Alberta clipper. *Wea. Forecasting,* **22,** 315–333, doi:10.1175/WAF982.1.

Zhang, X., J. E. Walsh, J. Zhang, U. S. Bhatt, and M. Ikeda, 2004: Climatology and interannual variability of Arctic cyclone activity: 1948–2002. *J. Climate,* **17,** 2300–2317, doi:10.1175/1520-0442(2004)017<2300:CAIVOA>2.0.CO;2.